Journal of Non-Newtonian Fluid Mechanics, 19 (1985) 15–41
Elsevier Science Publishers B.V., Amsterdam – Printed in The Netherlands

HYPERBOLICITY AND CHANGE OF TYPE IN THE FLOW OF VISCOELASTIC FLUIDS THROUGH CHANNELS

J.Y. YOO

Department of Mechanical Engineering, Seoul National University, Seoul (Korea)

and D.D. JOSEPH

Department of Aerospace Engineering and Mechanics, University of Minnesota, Minneapolis, Minnesota 55455 (U.S.A.)

(Received February 5, 1985)

Summary

We consider steady flow of an upper convected Maxwell fluid through a channel with wavy walls. The vorticity of this flow will change type when the velocity in the center of the channel is larger than a critical value defined by the propagation of shear waves. There is then a central region of the channel in which the vorticity equation is hyperbolic and a low speed region near the walls where the vorticity equation is elliptic. We linearize the problem for small amplitude waviness and the linearized problem is solved in detail. The characteristic nets depend on the viscoelastic "Mach" number which is the ratio ($M = U/c$) of the unperturbed maximum velocity U to the speed of shear waves c into the fluid at rest and the elasticity number E. There is a supercritical (hyperbolic) region around the center of the channel when $M > 1$. When $M \gg 1$, the thickness of this hyperbolic region is small when E is large, and large when E is small. Regions of positive and negative vorticity are swept out along forward facing characteristics in the hyperbolic region. There is rapid damping of vorticity in the hyperbolic region away from the boundary when $M \gg 1$ and the Weissenberg number $W = M\sqrt{E} \leqslant 0(1)$. (The Weissenberg number is proportional to the relaxation time of the fluid.)

The rate of damping of vorticity decreases as W is increased. Flows with high M appear to be more "elastic" when W is large in the sense that the damping is suppressed as the relaxation time of the fluid is increased.

0377-0257/85/$03.30

Introduction

This paper is the third in a series which addresses the analogue of the "transonic" problem of aerodynamics which arises in the problem of steady flow of viscoelastic liquids. This problem is associated with the fact that the equations governing the distribution of vorticity in steady flow can change type [1]; the flow is then partitioned into subcritical (elliptic) and supercritical (hyperbolic) regions for vorticity in a manner which has some analogies with the partitioning of high speed flow of gases into sub and supersonic regions. The viscoelastic problem is a very new one; there are only five papers: Rutkevich [2,3], Ultman and Denn [4], Luskin [5] and Yoo et al. [6]. Many curious, unexplained phenomena of the flow of viscoelastic fluids may have their origin in the transition from sub- to supercritical flow. In this series of papers we try to move the theory closer to physics by emphasizing issues which bear on the explanation of observations. The obstacles which we encounter are partly theoretical, having to do with the fact that the nonlinear theory is not yet well developed, particularly with respect to the development of shocks. Another theoretical problem has to do with constitutive equations. It can be shown [1,3] that conditions for hyperbolicity and changing type are very sensitive to the choice of constitutive equations. Only those constitutive models which have instantaneous elasticity will lead to quasilinear systems with real characteristic directions.

Fluids with instantaneous elasticity have no instantaneous viscosity in the same way that Maxwell models have no instantaneous viscosity and Jeffreys models do. The most general class of simple fluids with instantaneous elasticity is the class of fluids with fading memory of the Coleman–Noll type (see [7]). Probably most fluids have some viscous response and fluids with pure instantaneous elasticity are probably rare. Small viscosities lead to local smoothing and do not change the essential dynamics of fluids with large instantaneous elasticity (see [7–9]). It follows that the analysis of fluids with instantaneous elasticity ought to apply to many real fluids. However, the physical consequences of this type of analysis are not yet well understood. In our effort to understand what is changing type and where it is changing type we have been forced to use special models. This is unfortunate because we are uncertain whether the results of the analysis are intrinsic or whether they will change from model to model.

Joseph et al. [1] have given some elements of a general theory of constitutive equations of rate type for fluids with instantaneous elasticity. They show that the equation for vorticity of steady flows may change type from elliptic to hyperbolic as the speed is increased. The type of the equation may change in steady flow; but only for some models, not all, is it precisely the vorticity which changes type. The class of models for which the vorticity changes type

includes the family of Oldroyd models with zero retardation times (various Maxwell models) and some other special forms of single integral models; for example, BKZ models with constant coefficients. In other models, something other than the vorticity can change type.

Yoo et al. [6] tried to explain the striking experimental results of Metzner et al. [10] with an analysis of the vorticity perturbing irrotational sink flow. This type of sink flow was observed in conical region associated with flow into a hole. The analysis is based on the aforementioned family of Oldroyd models of Maxwell type with instantaneous elasticity. Despite some rather striking agreements between theory and experiment, it is necessary to maintain reservations both about the theory and the experiment. The constitutive equations used in the analysis are, at least, of uncertain validity, the assumptions of the analysis are without justification and the experiment is the only one in which a region of constant vorticity which is not a uniform motion is clearly identified.

It is against this background of uncertainty about the dynamics of vorticity in the flow of viscoelastic fluids that we note that the vorticity of all flows of fluids with instantaneous elasticity which perturb rigid motions will change type.

Our present effort is in a rather different direction. We are going to work with one special Oldroyd fluid, the upper convected Maxwell model, but we shall solve a definite (but linearized) problem of change of type in detail. To our knowledge this is the first time such a solution has been given. Such solutions can be computed using other models by the methods of this paper.

The problem of flow of non − Newtonian fluids through corrugated pipes was considered by Dodson et al. [11]. They also did experiments. They did not consider the problem of hyperbolicity and change of type. They used fluid models with effective viscosity (a retardation time) in their numerical computation. The effective viscosity has a smoothing effect. They worked at very low Reynolds numbers. Even if their retardation time (λ_2) is put to zero most of their computations are for subcritical flow.

2. Governing equations for steady flow of Maxwell fluid

We consider the steady flow of an upper convected Maxwell fluid through a plane channel with wavy walls as sketched in Fig. 2.1. The governing equations for this flow are

$$\operatorname{div} \boldsymbol{u} = 0, \tag{2.1a}$$

$$\rho\left[\frac{\partial \boldsymbol{u}}{\partial t} + \boldsymbol{u}\cdot\nabla\boldsymbol{u}\right] = -\nabla p + \nabla\cdot\tau, \tag{2.1b}$$

$$\lambda\left[\frac{\partial \tau}{\partial t} + \boldsymbol{u}\cdot\nabla\tau - \nabla u\cdot\tau - \tau\cdot\nabla u^{\mathrm{T}}\right] + \tau = \eta(\nabla\boldsymbol{u} + \nabla\boldsymbol{u}^{\mathrm{T}}). \tag{2.1c}$$

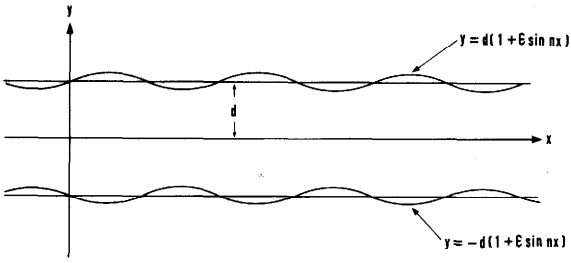

Fig. 2.1. Schematic diagram of plane channel with wavy walls.

where ρ is the density, λ is the stress relaxation time, η is the zero shear rate viscosity, t is the time, $\boldsymbol{u}$ is the velocity, p is the constitutively indeterminate part of the Cauchy stress tensor and τ is the determinate part.

Other symbols used in the analysis are listed below:

(x, y)	rectangular Cartesian coordinate
d	half of the mean channel depth
U_*	centerplane velocity
(u, v)	physical components of velocity
(σ, γ, τ)	physical components of stress $= (\tau_{xx}, \tau_{yy}, \tau_{xy})$
μ	η/λ
R	Reynolds number $= \rho U_* d/\eta$
W	Weissenberg number $= U_*\lambda/d$
E	Elasticity number $= \eta\lambda/\rho d^2$
M	Viscoelastic Mach number $= U_*/(\eta/\lambda\rho)^{1/2}$

Only two of the parameters R, W, E, M appear in the analysis. We shall express our results in terms of E and M. E is a material parameter independent of the motion. M, the viscoelastic "Mach" number, is linear in U_*. The shear wave speed is a material parameter

$$c = (\eta/\lambda p)^{1/2},$$

which is fixed by the fluid. Of course, R and W can be expressed in terms of E and M

$$RW = M^2, \quad W = RE, \quad R = M/\sqrt{E}, \quad W = M\sqrt{E}.$$

In considering various limits of parameters it is helpful to note that when the viscosity and relaxation time λ tend to zero in such a way that η/λ is finite, c remains finite but $E \to 0$.

Newtonian fluids arise in the limit $c \to \infty$, $M \to 0$, $E \to 0$ in such a way that $R = M/\sqrt{E}$ is finite.

Flows which perturb uniform motions go supercritical when $M > 1$. Wave speeds for water based polymer solutions are of the order 1 cm/s or 10

cm/s. The wave speeds of polymer melts are of the order of 100 cm/s. At the same time, the large viscosities of melts reduce the possibility of achieving large velocities. Hence for the flow of melts we expect that the flow is usually subcritical $M < 1$. On the other hand, in water based polymers of the kind which are effective in drag reduction, we expect to see many flows with $M > 1$.

The parameters M and E appear in the dimensionless equations (2.2) which arise from (2.1) when d, U_*, η/λ are introduced as scales for length, velocity and stress.

$$u_x + v_y = 0, \tag{2.2a}$$

$$uu_x + vu_y + \frac{1}{M^2}(p_x - \sigma_x - \tau_y) = 0, \tag{2.2b}$$

$$uv_x + vv_y + \frac{1}{M^2}(p_y - \tau_x - \gamma_y) = 0, \tag{2.2c}$$

$$u\sigma_x + v\sigma_y - 2(\sigma + 1)u_x - 2\tau u_y = -\frac{\sigma}{M\sqrt{E}}, \tag{2.2d}$$

$$u\tau_x + v\tau_y - (\gamma + 1)u_y - (\sigma + 1)v_x = -\frac{\tau}{M\sqrt{E}}, \tag{2.2e}$$

$$u\gamma_x + v\gamma_y - 2\tau v_x - 2(\gamma + 1)v_y = -\frac{\gamma}{M\sqrt{E}}. \tag{2.2f}$$

We shall seek and find a solution of these equations satisfying no slip conditions at the walls

$$u = v = 0 \text{ at } y = \pm(1 + \epsilon \sin nx) \tag{2.3}$$

with symmetric streamlines

$$\frac{\partial u}{\partial y} = v = 0 \text{ at } y = 0. \tag{2.4}$$

It is noteworthy that our solution is completely determined by data (2.3) and (2.4) on the velocity alone. It is not necessary, and it would be wrong to prescribe more about velocity or stresses.

3. The vorticity equation

Flows of incompressible fluids in the vertical plane are conveniently represented by a streamfunction $\psi(x, y)$

$$(u, v) = \left[\frac{\partial \psi}{\partial y}, -\frac{\partial \psi}{\partial x}\right].$$

The vorticity $\omega = \text{curl } \boldsymbol{u}$ is related to the streamfunction

$$\omega = \text{curl } \boldsymbol{u} = \omega \boldsymbol{e}_z = -\left[\frac{\partial^2 \psi}{\partial x^2} + \frac{\partial^2 \psi}{\partial y^2}\right]\boldsymbol{e}_z, \tag{3.1}$$

where $\omega(x, y)$ satisfies

$$(M^2u^2 - \sigma - 1)\omega_{xx} + 2(M^2uv - \tau)\omega_{xy} + (M^2v^2 - \gamma - 1)\omega_{yy}$$
$$+\left[-p_x + \frac{M}{\sqrt{E}}u\right]\omega_x + \left[-p_y + \frac{M}{\sqrt{E}}v\right]\omega_y$$
$$+(u_x - v_y)(\sigma_{xy} + \gamma_{xy} + \tau_{xx} + \tau_{yy}) + (u_y + v_x)(\gamma_{yy} - \sigma_{xx})$$
$$+\sigma_y u_{xx} + 2\tau_y u_{xy} + \gamma_y u_{yy} - \sigma_x v_{xx} - 2\tau_x v_{xy} - \gamma_x v_{yy} = 0. \tag{3.2}$$

Equation (3.2) may be written as

$$A\omega_{xx} + 2B\omega_{xy} + C\omega_{yy} + \text{l.o.t} = 0, \tag{3.3}$$

where the terms l.o.t. are of lower order for hyperbolic analysis (see [1]). Characteristic directions

$$\frac{dy}{dx} = \frac{B}{A} \pm \frac{\sqrt{B^2 - AC}}{A},$$
$$A = M^2u^2 - \sigma - 1,$$
$$B = M^2uv - \tau,$$
$$C = M^2v^2 - \gamma - 1 \tag{3.4}$$

for the vorticity exist whenever

$$\Sigma \overset{\text{def}}{=} \tau^2 - 2M^2\tau uv - (1 + \gamma)(1 + \sigma) + M^2v^2(1 + \sigma) + M^2u^2(1 + \gamma) > 0. \tag{3.5}$$

The expression (3.5) is expressed in terms of unknown velocity and stress fields. The criterion (3.5) for hyperbolicity can be satisfied in some regions of flow and not in others. The border $\Sigma = 0$ between the elliptic and hyperbolic regions of flow is like the sonic line in gas dynamics. Across this line the equations are said to change type.

Equation (2.2) and all the equations of this section are general in that they apply to every plane problem, not just the channel flow problem introduced in Section 1.

4. Characteristics nets for problems perturbing plane Poiseuille flow

Now we shall solve the governing equations for flow in a channel with straight walls $\epsilon = 0$:

$$(u_0, v_0) = (1 - y^2, 0), \quad (p_0, \tau_0) = -2M\sqrt{E}(x, y),$$
$$(\sigma_0, \gamma_0) = (8M^2Ey^2, 0), \quad \omega_0 = 2y. \tag{4.1}$$

The basic motion depends exclusively on the Weissenberg number $W = M\sqrt{E}$

measuring the size of stresses. The solution (4.1) is relatively featureless and, in particular, it gives no indication of hyperbolicity.

Now we consider any plane perturbation of (4.1). The problem with wavy walls is one such perturbation, but there are infinitely many others. We may linearize the formula (3.4) for the characteristics of *any* flow slightly perturbing the Poiseuille flow (4.1). The characteristics for all these perturbations

$$\frac{dy}{dx} = \frac{1}{M}\left[\frac{-2\sqrt{E}\,y \pm \sqrt{(y^2-1)^2 - 4Ey^2 - M^{-2}}}{-(y^2-1)^2 + 8Ey^2 + M^{-2}}\right] \tag{4.2}$$

are defined in terms of quantities defined for the basic flow (4.1) and are given once and for all, independent of the perturbation.

Equation (4.2) shows that flows perturbing plane Poiseuille flow can exhibit a change of type with a "sonic" line $\Sigma = 0$ given by

$$\Sigma(y^2) = (y^2-1)^2 - 4Ey^2 - M^{-2} = 0 \quad (-1 \leqslant y \leqslant 1).$$

Since $\Sigma(y^2)$ is monotonically decreasing, it has a maximum at $y^2 = 0$ and

$$\Sigma(0) = 1 - M^{-2} > 0$$

if and only if the viscoelastic "Mach" number $M > 1$. The "sonic" line across which the flow changes type is $y = y^*$ where $\Sigma(y^{*2}) = 0$,

$$y^* = \pm\left[1 + 2E - 2\left[E^2 + E + \frac{1}{4M^2}\right]^{1/2}\right]^{1/2}.$$

In thinking about the regions of hyperbolicity and characteristics nets it is useful to consider the strongly supercritical case $M \gg 1$. Then, when E is small, we obtain

$$y^* = \pm(1 - 2\sqrt{E})^{1/2} \tag{4.3}$$

and the elliptic region $y^* \leqslant y \leqslant 1$ is near the wall $y = \pm 1$. Most of the flow is hyperbolic. On the other hand, when E is larger, we get

$$y^* = \pm\left[1 + 2E - 2E[1 + 1/E]^{1/2}\right]^{1/2} = \pm O[1/E]^{1/2} \tag{4.4}$$

and the hyperbolic region $0 \leqslant y \leqslant y^*$ is confined to a small strip centered on the center of the channel.

The two families of characteristics defined by (4.2) enter the region of hyperbolicity from the elliptic strip on the wall with the same slope

$$\left[\frac{dy}{dx}\right]_{y=y^*} = -\frac{1}{2M\sqrt{E}\,y^*} = -\frac{1}{2Wy^*}. \tag{4.5}$$

This common entering slope of the two families of characteristics is propor-

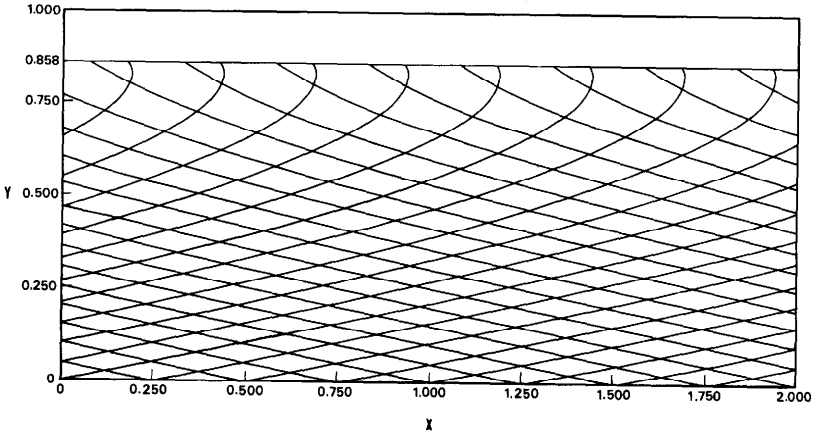

Fig. 4.1. Characteristics net for $E = 0.0100$ and $M = 5.0$, $(R, W) = (50, 0.5)$.

tional to the reciprocal of the Weissenberg number. One of the two families of characteristics has an infinite slope at the zero of the denominator in (4.2). This family changes slope, has a turning point, at this zero. The other family $(+)$ is monotone because the numerator in (4.2) vanishes at the same value of y as the denominator. The slopes of the characteristics tend to zero for each fixed E as $M \to \infty$ except near the turning point of the $(-)$ family of characteristics.

In Figs. 4.1–4.8 we have exhibited the characteristics nets for different values of E and M. The graphs were obtained by numerical integration of (4.2). The computer graphics are not sufficiently fine to bring out the feature

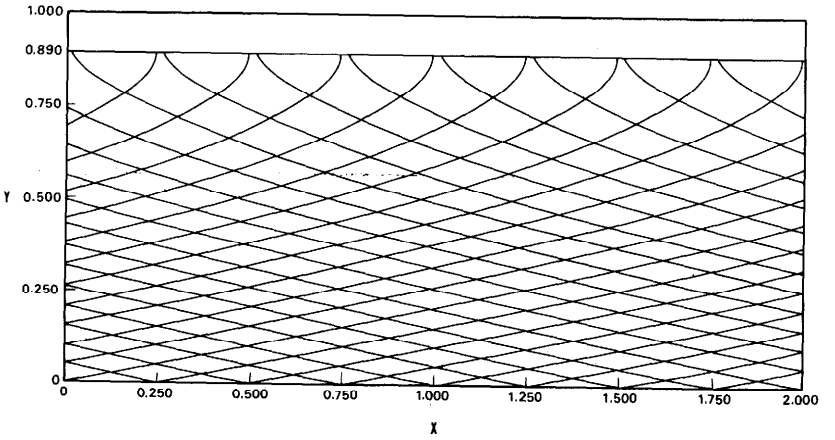

Fig. 4.2. Characteristics net for $E = 0.0010$ and $M = 5.00$, $(R, W) = (158.1, 0.158)$.

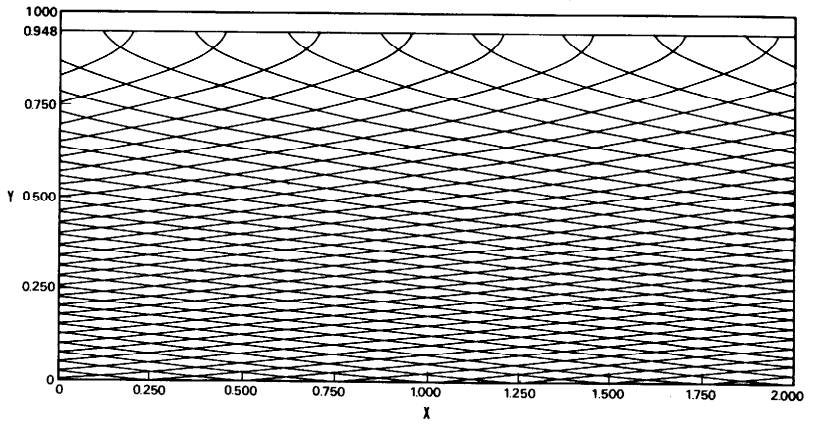

Fig. 4.3. Characteristics net for $E = 0.0001$ and $M = 10.00$, $(R, W) = (1000, 0.01)$.

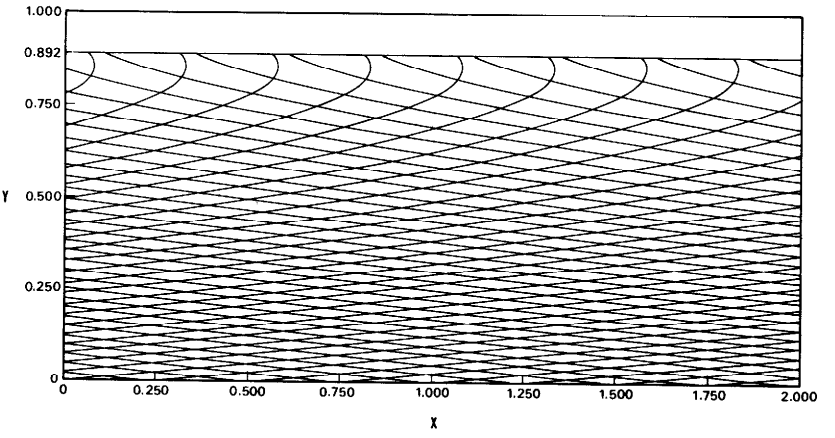

Fig. 4.4. Characteristics net for $E = 0.0100$ and $M = 10.0$, $(R, W) = (100, 1)$.

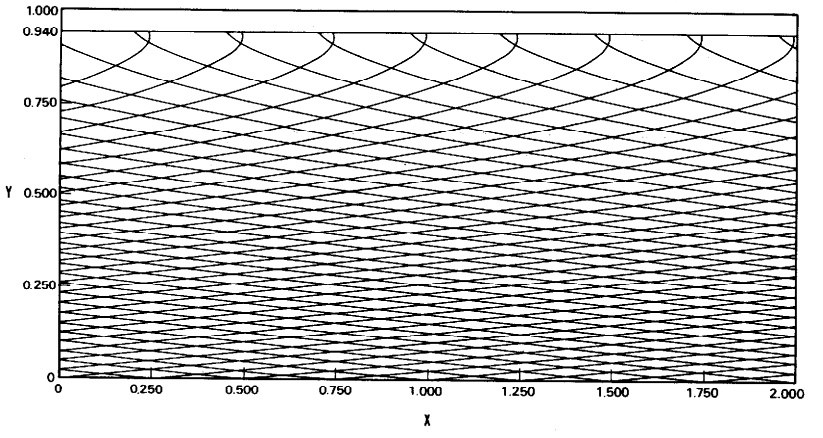

Fig. 4.5. Characteristics net for $E = 0.0010$ and $M = 10.00$, $(R, W) = (316.2, 0.316)$.

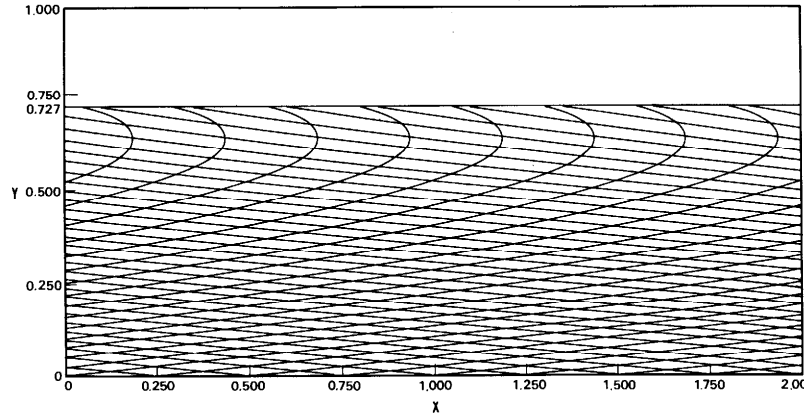

Fig. 4.6. Characteristics net for $E = 0.1000$ and $M = 10.0$, $(R, W) = (31.6, 3.16)$.

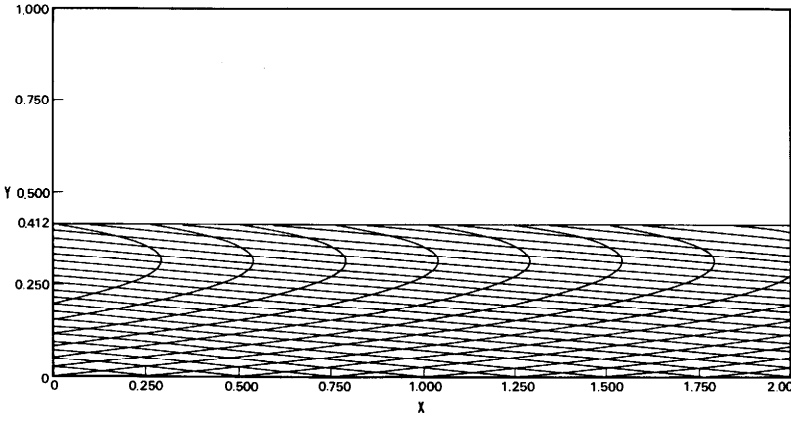

Fig. 4.7. Characteristics net for $E = 1.0000$ and $M = 10.0$, $(R, W) = (10, 10)$.

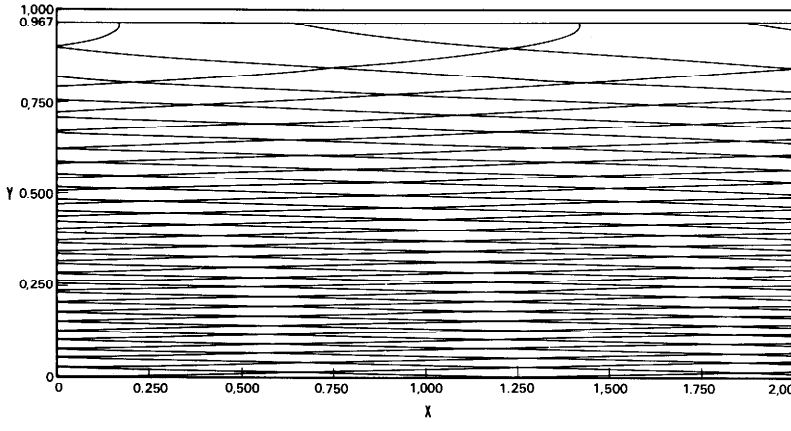

Fig. 4.8. Characteristics net for $E = 0.0010$ and $M = 50.00$, $(R, W) = (1581, 1.581)$.

that the entering slope of families of characteristics have a common value at the "sonic" line.

We emphasize again that these characteristics are universal in the sense that they hold for every linearized problem perturbing plane Poiseuille flow. To go further we must choose a specific perturbation and solve a definite boundary value problem. In the next section we undertake to solve the linearized problem associated with Fig. 2.1.

5. Perturbation equations for wavy walls

We return to the problem of flow in channels with wavy walls which was introduced in Section 1 and study it using a method of domain perturbations in the amplitude ϵ of the waviness of the wall (see [12] for a similar application). We define a one-to-one mapping

$$x = x_0, \quad y = y_0(1 + \epsilon \sin nx_0) \tag{5.1}$$

of the wavy domain

$$V_\epsilon\colon\ -1 - \epsilon \sin nx \leqslant y \leqslant 1 + \epsilon \sin nx, \quad -\infty < x < \infty$$

into the flat domain

$$V_0\colon\ -1 \leqslant y \leqslant 1, \quad -\infty < x < \infty,$$

and we seek a solution of (2.2,3,4) by expanding $[u, v, p, \sigma, \gamma, \tau](x, y, \epsilon)$ and $y(\epsilon)$ in powers of ϵ. The solution at zeroth order is the Poiseuille flow (4.1). For example

$$u(x, y, \epsilon) = u_0(x_0, y_0) + \epsilon u^{[1]}(x_0, y_0) + 0(\epsilon^2).$$

The function $u^{[1]}(x_0, y_0)$ is a derivative with respect to ϵ at $\epsilon = 0$ holding y_0 fixed. After applying the chain rule, we get

$$u^{[1]}(x_0, y_0) = u^{\langle 1\rangle}(x_0, y_0) + \left.\frac{\partial y}{\partial \epsilon}\right|_{(\epsilon=0)} \frac{\partial u_0}{\partial y_0},$$

where

$$\frac{\partial y}{\partial \epsilon} = y_0 \sin nx_0. \tag{5.2}$$

The field $u^{\langle 1\rangle}(x_0, y_0)$ is a partial derivative holding y fixed (and equal to y_0).

We are going to compute the derivatives $[u^{\langle 1\rangle}, v^{\langle 1\rangle}, p^{\langle 1\rangle}, \sigma^{\langle 1\rangle}, \gamma^{\langle 1\rangle}, \tau^{\langle 1\rangle}]$ from a linearized boundary value problem. After finding these fields we may express the solution in the deformed domain V_ϵ by inverting the mapping.

For simplicity in notation we now drop the superscript $\langle 1\rangle$ and find that

$$u_x + v_y = 0, \tag{5.3a}$$

$$(1-y^2)u_x - 2yv + \frac{1}{M^2}(p_x - \sigma_x - \tau_y) = 0, \tag{5.3b}$$

$$(1-y^2)v_x + \frac{1}{M^2}(p_y - \tau_x - \gamma_y) = 0, \tag{5.3c}$$

$$(1-y^2)\sigma_x + 16M^2Eyv - 2(8M^2Ey^2+1)u_x + 4y\tau + 4M\sqrt{E}\,yu_y + \sigma/M\sqrt{E} = 0, \tag{5.3d}$$

$$(1-y^2)\gamma_x + 4M\sqrt{E}\,yv_x - 2v_y + \gamma/M\sqrt{E} = 0, \tag{5.3e}$$

$$(1-y^2)\tau_x - 2M\sqrt{E}\,v + 2y\gamma - (8M^2Ey^2+1)v_x - u_y + \tau/M\sqrt{E} = 0, \tag{5.3f}$$

where

$$u(x,\pm 1) = 2\sin nx,$$

$$v(x,\pm 1) = 0,$$

$$v(x,0) = u_y(x,0) = 0. \tag{5.4}$$

We can solve the equations (5.3) using only the velocity data (5.4).

The velocity can be obtained from a stream function $\psi(x, y)$

$$(u, v) = (\psi_y, -\psi_x).$$

The vorticity

$$\omega^{\text{def}} = v_x - u_y = -\nabla^2\psi \tag{5.5}$$

satisfies an equation

$$\left[(1-y^2)^2 - 8Ey^2 - \frac{1}{M^2}\right]\omega_{xx} + 4\frac{\sqrt{E}}{M}y\omega_{xy} - \frac{\omega_{yy}}{M^2} + \left[\frac{2\sqrt{E}}{M} + \frac{1}{M\sqrt{E}}(1-y^2)\right]\omega_x = \frac{-2v}{M\sqrt{E}} - 16Eyu_{xx} + \frac{4\sqrt{E}}{M}u_{xy} - 2(1-y^2)v_x + \frac{1}{M^2}\left[2\tau_x + 2y\gamma_{yy} - 2y\sigma_{xx} + 4\gamma_y\right] \tag{5.6}$$

of changing type whose characteristics are given by (3.4)

6. Separation of variables

The column vector $\boldsymbol{q}$ with components $[u, v, p, \sigma, \gamma, \tau]$ satisfies a linear system

$$\boldsymbol{A}(y)\boldsymbol{q}_x + \boldsymbol{B}(y)\boldsymbol{q}_y = \boldsymbol{C}(y)\boldsymbol{q}. \tag{6.1}$$

The boundary conditions (5.4), linearity and the fact that the coefficients of the linear equation are independent of x, imply that

$$\boldsymbol{q}(x, y) = \boldsymbol{q}_1(y) \cos nx + \boldsymbol{q}_2(y) \sin nx. \tag{6.2}$$

The existence of eigensolutions of (6.1) can be ruled out by a stability argument when M and W are both small. In this argument we establish that the rest state is stable. All the variables of the linearized problem have a decomposition like (6.2).

We insert the decomposition (6.2) into the equation (6.1), where $\boldsymbol{A}(y)$, $\boldsymbol{B}$(y), $\boldsymbol{C}$(y) are defined by (5.3), and we put the coefficients of cos nx and sinnx to zero. As a result, we obtain a system of 12 ordinary differential equations of the form

$$\begin{bmatrix} \boldsymbol{B} & \boldsymbol{0} \\ \boldsymbol{0} & \mathbf{B} \end{bmatrix} \begin{bmatrix} \boldsymbol{q}_1'(y) \\ \boldsymbol{q}_2'(y) \end{bmatrix} - \begin{bmatrix} \boldsymbol{C} & -n\boldsymbol{A} \\ n\boldsymbol{A} & \boldsymbol{C} \end{bmatrix} \begin{bmatrix} \boldsymbol{q}_1(y) \\ \boldsymbol{q}_2(y) \end{bmatrix} = \boldsymbol{0}, \tag{6.3}$$

which can be solved sequentially in terms of $v_1(y)$, $v_2(y)$ and their derivatives. By "sequentially" we mean that (u_1, u_2), (γ_1, γ_2), (τ_1, τ_2), (σ_1, σ_2) and (p_1, p_2) are found in that order as functions of v_1, v_2 and their derivatives. We may then obtain two equations for v_1 and v_2 (or ψ_1 and ψ_2) by differentiating p_1 and p_2, and equating these two derivatives to their expressions (p_1', p_2') as given by the equations (5.3c). In this way we come up with the two fourth order differential equations for ψ_1 and ψ_2 given below:

$$\begin{aligned} \psi_1^{iv} &= A_{11}\psi_1''' + A_{12}\psi_2''' + A_{21}\psi_1'' + A_{22}\psi_2'' \\ &\quad + A_{31}\psi_1' + A_{32}\psi_2' + A_{41}\psi_1 + A_{42}\psi_2, \\ \psi_2^{iv} &= -A_{12}\psi_1''' + A_{11}\psi_2''' - A_{22}\psi_1'' + A_{21}\psi_2'' \\ &\quad - A_{32}\psi_1' + A_{31}\psi_2' - A_{42}\psi_1 + A_{41}\psi_2, \end{aligned} \tag{6.4}$$

where, denoting

$$X = \frac{M^2E}{1 + M^2En^2(1-y^2)^2},$$

$$A_{11} = X\left[-4n^2y(1-y^2)\right],$$

$$A_{12} = X\left[4M\sqrt{E}\,n^3y(1-y^2)^2\right],$$

$$A_{21} = n^2\left[-M^2(1-y^2)^2 + 2 + 6M^2Ey^2\right] + Xn^2\left[-6 + 2M^2En^2y^2(1-y^2)^2\right] + X^2\left[-16n^4y^2(1-y^2)^2\right],$$

$$A_{22} = \frac{M}{\sqrt{E}} n(1-y^2) + 6X\left[M\sqrt{E}\, n^3(1-y^2)^2\right] + X^2\left[16M\sqrt{E}\, n^5 y^2(1-y^2)^3\right],$$

$$A_{31} = Xn^4\left[4y(1-y^2) + 16M^2Ey(1-y^4)\right] + X^2\left[-32n^4y(1-y^4)\right],$$

$$A_{32} = X\left[-4M\sqrt{E}\, n^5 y(1-y^2)^2\right] + X^2\left[32M\sqrt{E}\, n^5 y(1-y^2)(1-y^4)\right],$$

$$\begin{aligned} A_{41} = {} & n^2\left[-2M^2(1-y^2) + n^2M^2(1\text{-}y^2)^2 - n^2\right] \\ & + Xn^2\left[-12 + 2n^2(1-y^2) + 48M^2En^2y^2\right. \\ & \left. - 16M^2En^2y^4 - 8M^2En^4y^2(1-y^2)^2\right] \\ & + X^2n^4\left[-96y^2 - \frac{16}{M^2E}y^2 + 32M^2En^2y^4(1-y^2)^2\right], \end{aligned}$$

$$\begin{aligned} A_{42} = {} & 2\frac{M}{\sqrt{E}}n - \frac{M}{\sqrt{E}}n^3(1-y^2) \\ & + Xn^3\left[-2M\sqrt{E}\, n^2(1-y^2)^2 - 44M\sqrt{E}\, y^2 + 12M\sqrt{E}\right] \\ & + X^2n^3\left[128M\sqrt{E}\, n^2y^2(1-y^2) + \frac{16}{M\sqrt{E}}n^2y^2(1-y^2) + \frac{32}{M\sqrt{E}}y^2\right]. \end{aligned}$$

The boundary conditions are

$$\psi_1(0) = \psi_1''(0) = \psi_2(0) = \psi_2''(0) = \psi_1(1) = \psi_1'(1) = \psi_2(1) = 0,$$
$$\psi_2'(1) = 2. \tag{6.5}$$

The perturbed vorticity $\omega(x, y) = -\nabla^2\psi$ can be obtained from $\psi_1(y)$ and $\psi_2(y)$

$$\omega(x, y) = \left[-\psi_1''(y) + n^2\psi_1(y)\right]\cos nx + \left[-\psi_2''(y) + n^2\psi_2(y)\right]\sin nx. \tag{6.6}$$

Equations (6.4) and (6.5) can be solved by a standard shooting technique employing a fourth order Runge-Kutta method.

The numerical results will be given in Section 7. Nearly all of these are for $M \geqslant 5$. If we restrict our considerations to the case of large M with $W = M\sqrt{E} \leqslant O(1)$, we find that (6.4) may be written

$$\begin{aligned} & (1-y^2)^2n^2\psi_1^{(ii)} + \psi_1^{(iv)} - \frac{n}{M\sqrt{E}}\psi_2^{(ii)} \\ & = \frac{1}{M}\frac{4M^2En^2y(1-y^2)}{1 + M^2En^2(1-y^2)^2}\left(nM\sqrt{E}\,(1-y^2)\psi_2^{(iii)} - \psi_1^{(iii)}\right) + O\left[\frac{1}{M^2}\right] \end{aligned} \tag{6.7}$$

along with a second equation, say (6.8), which is the same as (6.7) when the subscripts 1 and 2 are interchanged and $-n$ replaces n. The derivatives in (6.7) are

$$\psi^{(\mathrm{i})} \overset{\text{def}}{=} \frac{1}{M}\psi'.$$

For large M, the vorticity is given by $\omega = -M^2\psi^{(\mathrm{ii})}$. If E is fixed and M is sufficiently large the vorticity in the interior of hyperbolic regions oscillates as y is increased from zero with a frequency given roughly by

$$\Omega = (1-y^2)Mn = (1-y^2)M2\pi N,$$

corresponding to half periods of oscillation given by

$$\frac{\pi}{\Omega} = \frac{1}{2(1-y^2)MN}.$$

This formula for successive zeroes of ω fits the numerical results well (e.g., see Figs. 7.2). When $E \to 0$ for fixed M we get $\psi_1'', \psi_2'' \to 0$ to leading order and the vorticity in the hyperbolic region tends to zero (e.g. see Fig. 7.9A).

7. Results

We shall display our numerical results in graphical form. We have three parameters M, E and the wave number n of the wavy wall. The characteristics for this problem are universal for all problems perturbing Poiseuille flow. Graphs of the characteristics as functions of E and M were given in Section 4.

A few preliminary remarks may help the reader to interpret the graphs shown in this section. It will be recalled that the boundary data which forces our problem is periodic in x with period $2\pi/n$. In fact the whole solution is periodic in x with period $2\pi/n$. Lines of zero vorticity separate regions of positive vorticity from regions of negative vorticity. The stream function is periodic in x in the same way. All the graphs cover one full period of the solution.

Our first observations are about the dependence of the solution on the wave number $n = 2\pi N$. Numerical computation with ever larger wave numbers (short waves) becomes increasingly difficult, first with slow convergence, then failure. For moderate and long waves ($N < 1$) we get good convergence. The solution does not seem to be very sensitive to changes in the wave number. Zero vorticity lines and characteristics are plotted on the same picture in each of the three cases, $N = 0.25$, $N = 0.50$, $N = 1.00$, represented in each of Figs. 7.1, 7.2, 7.3. The form of the zero vorticity line does not appear to depend strongly on n for $0.25 \leqslant N \leqslant 1$.

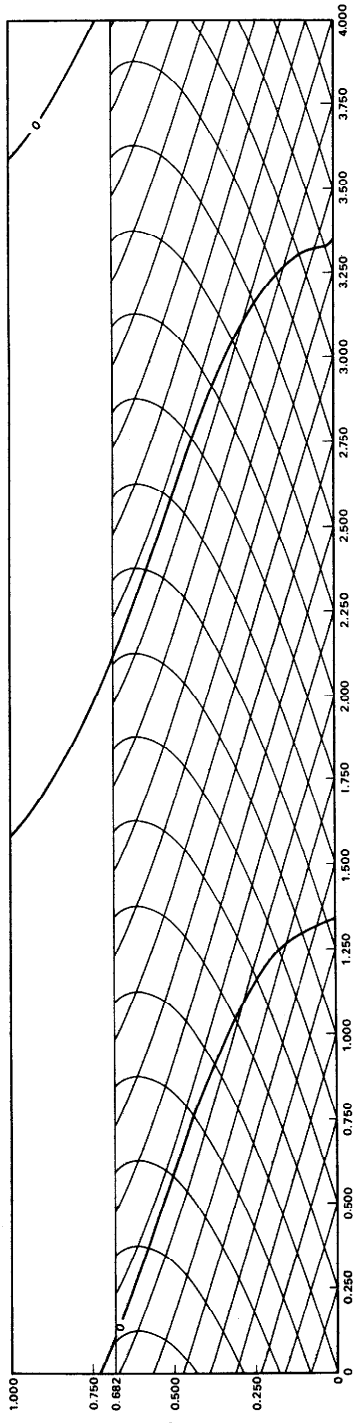

Fig. 7.1(a). Zero-vorticity curves for $E = 0.1000$, $M = 3.16$ and $N = 0.25$, $(R, W) = (10, 1)$.

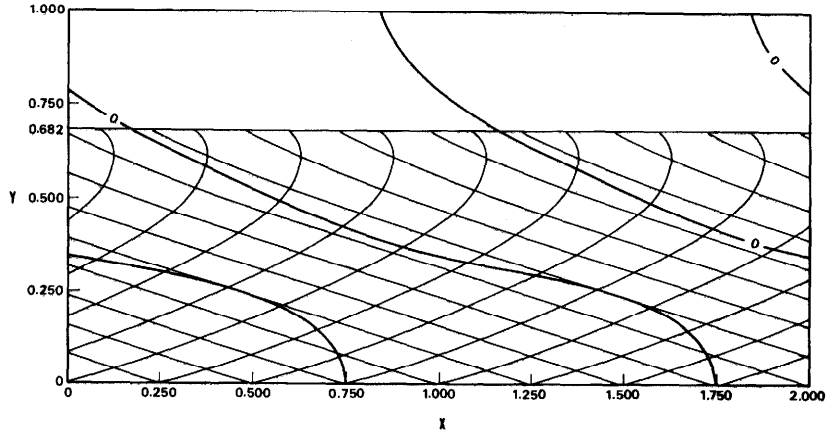

Fig. 7.1(b). Zero-vorticity curves for $E = 0.1000$, $M = 3.16$ and $N = 0.50$, $(R, W) = (10, 1)$.

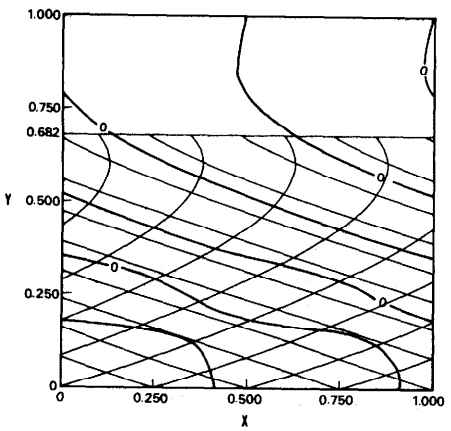

Fig. 7.1(c). Zero-vorticity curves for $E = 0.1000$, $M = 3.16$ and $N = 1.00$, $(R, W) = (10, 1)$.

The most striking feature of Figs. 7.1–7.3 is the way regions of positive and negative perturbed vorticity are swept out along characteristics. This sweeping property occurs in all the other supercritical cases computed by us. We have no good theoretical explanation of this property. The sweeping property, evident in the supercritical region is also evident in the subcritical region near the wall. It is apparent that in problems of change of type the supercritical flow will react with the subcritical flow so that the elliptic and hyperbolic regions of flow are compatible. We should get the same solution from a Cauchy problem set on the "sonic" line with the correct "initial conditions" taken from the compatible "true" solution. If regions of positive and negative data were then replaced with constant data having the same

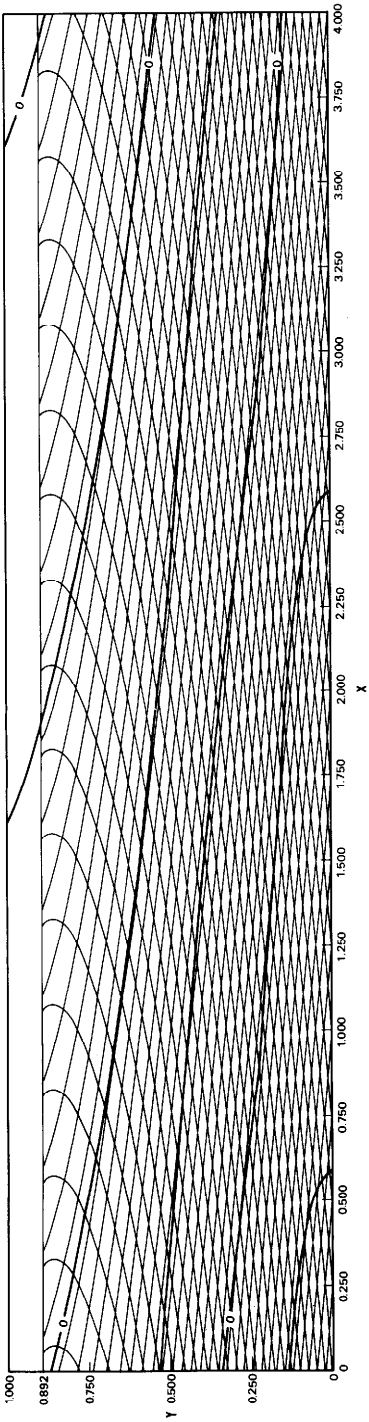

Fig. 7.2(a). Zero-vorticity curves for $E = 0.0100$, $M = 10.00$ and $N = 0.25$, $(R, W) = (100, 1)$.

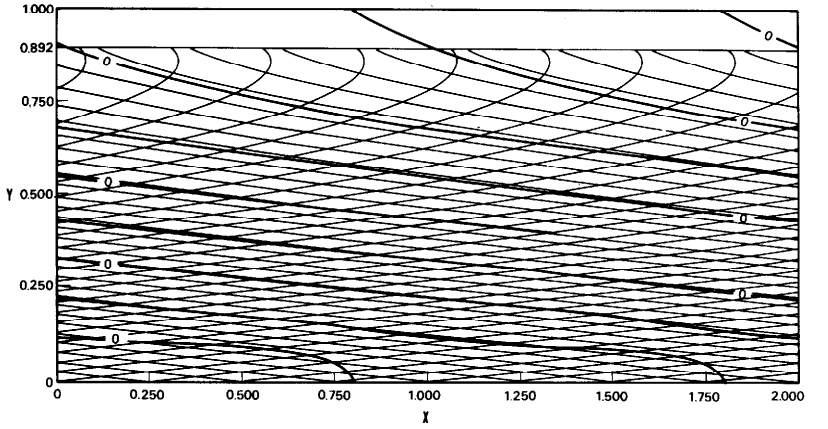

Fig. 7.2(b). Zero-vorticity curves for $E = 0.0100$, $M = 10.00$ and $N = 0.50$, $(R, W) = (100, 1)$.

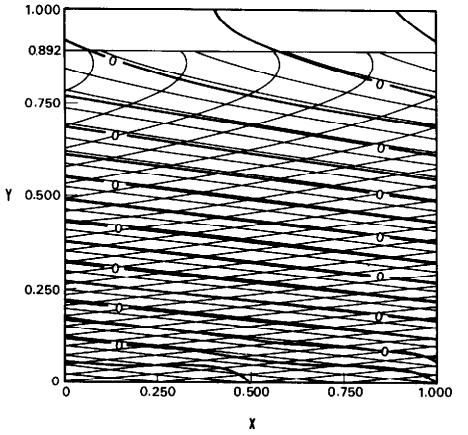

Fig. 7.2(c). Zero-vorticity curves for $E = 0.0100$, $M = 10.00$ and $N = 1.00$, $(R, W) = 100, 1)$.

mean value as true data we should have formed a Cauchy problem with approximating but discontinuous data, and the discontinuities would propagate along characteristics carrying regions of positive and negative perturbed vorticity between characteristics. In fact these regions of positive and negative perturbed vorticity would be damped, as in the true solution, with fast damping for low Weissenberg number fluids (small λ, short memory).

The graphs shown in Figs. 7.4–7.10 are computed for $N = 0.5$. In each figure there is (a) a plot of the iso-vorticity lines and (b) a plot of the streamlines. We are interested in how the solution varies with E and M. The reader should recall that the solution is periodic in x with period $2\pi/n$ and one period is on each graph.

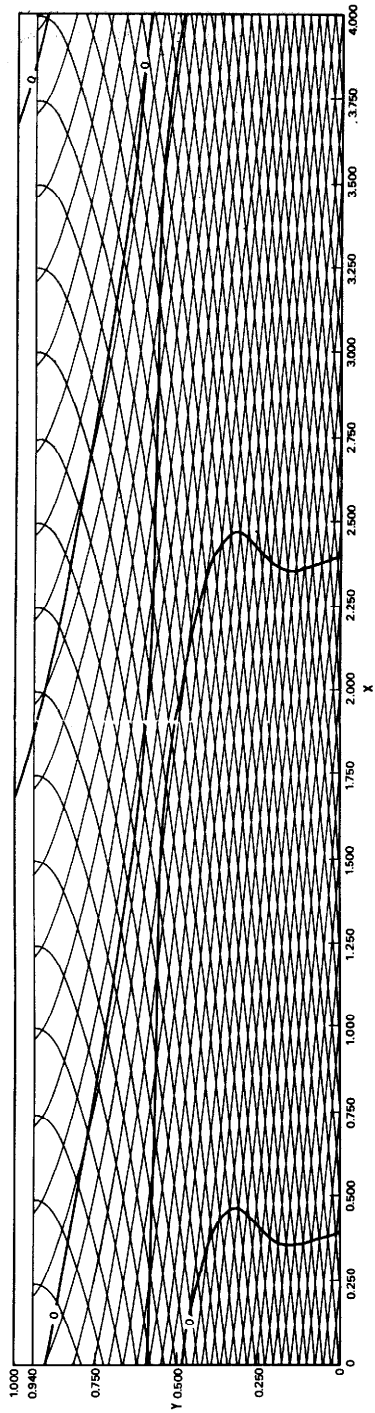

Fig. 7.3(a). Zero-vorticity curves for $E = 0.0010$, $M = 10.00$ and $N = 0.25$, $(R, W) = (316, 0.316)$.

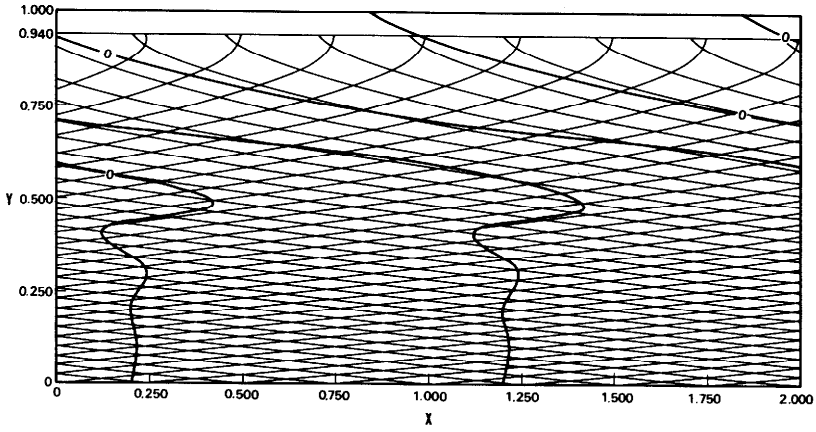

Fig. 7.3(b). Zero-vorticity curves for $E = 0.0010$, $M = 10.00$ and $N = 0.50$, $(R, W) = (316, 0.316)$.

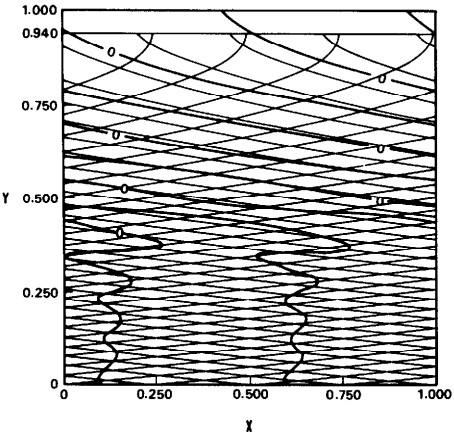

Fig. 7.3(c). Zero-vorticity curves for $E = 0.0010$, $M = 10.00$ and $N = 1.00$, $(R, W) = (316, 0.316)$.

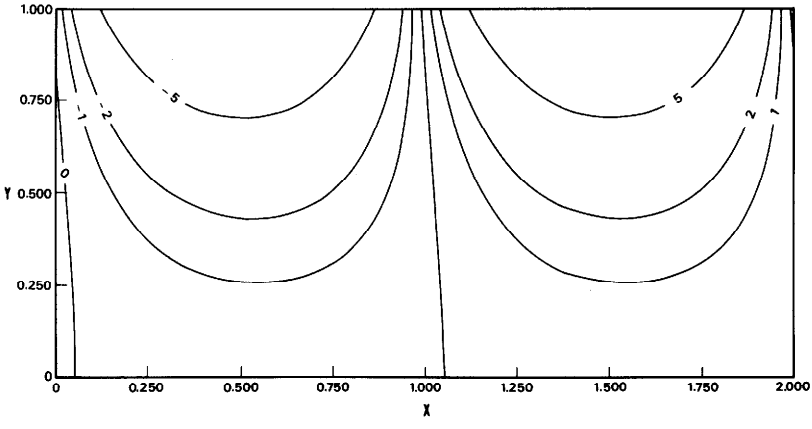

Fig. 7.4(a). Iso-vorticity curves for $E = 0.0100$, $M = 0.10$, $(R, W) = (1, 0.01)$.

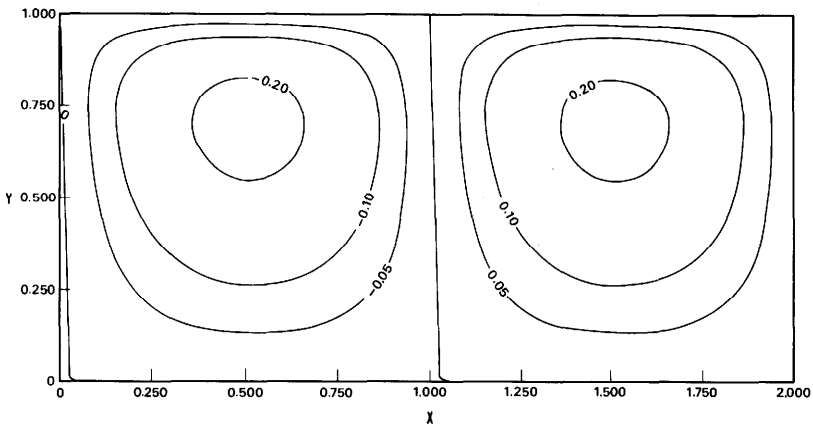

Fig. 7.4(b). Streamlines for $E = 0.0100$, $M = 0.10$, $(R, W) = (1, 0.01)$.

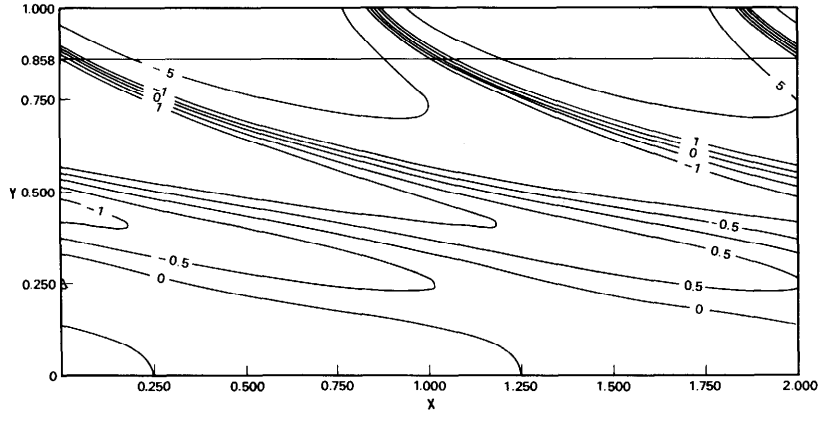

Fig. 7.5(a). Iso-vorticity curves for $E = 0.0100$, $M = 5.00$, $(R, W) = (50, 0.5)$.

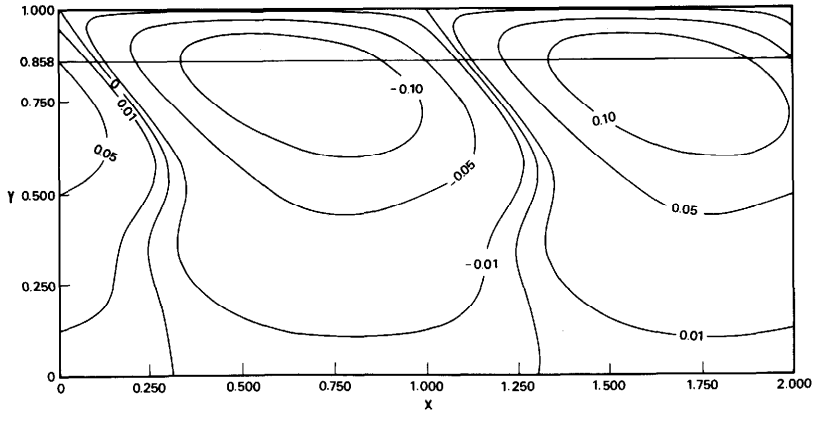

Fig. 7.5(b). Streamlines for $E = 0.0100$, $M = 5.00$, $(R, W) = (50, 0.5)$.

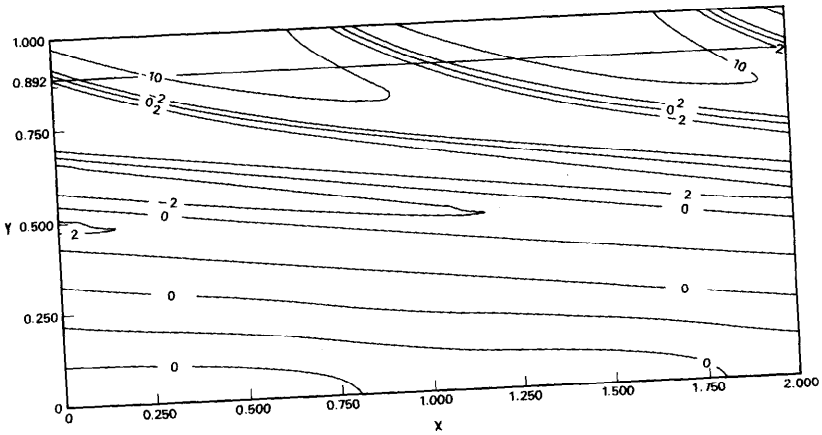

Fig. 7.6(a). Iso-vorticity curves for $E = 0.0100$, $M = 10.00$, $(R, W) = (100, 1)$.

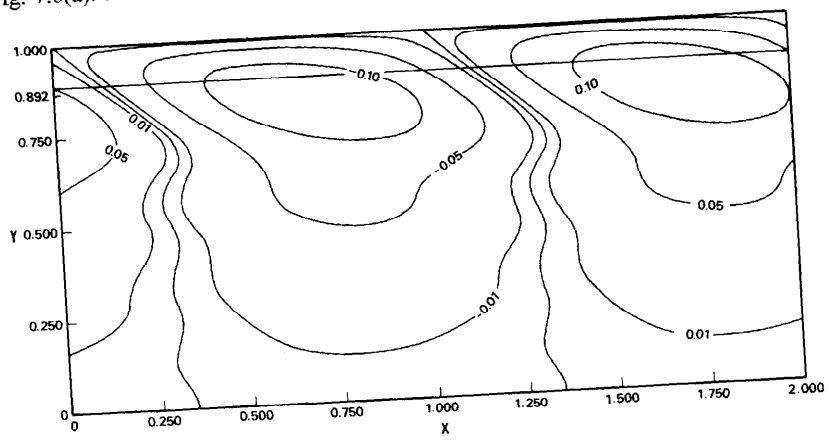

Fig. 7.6(b). Streamlines for $E = 0.0100$, $M = 10.00$, $(R, W) = (100, 1)$.

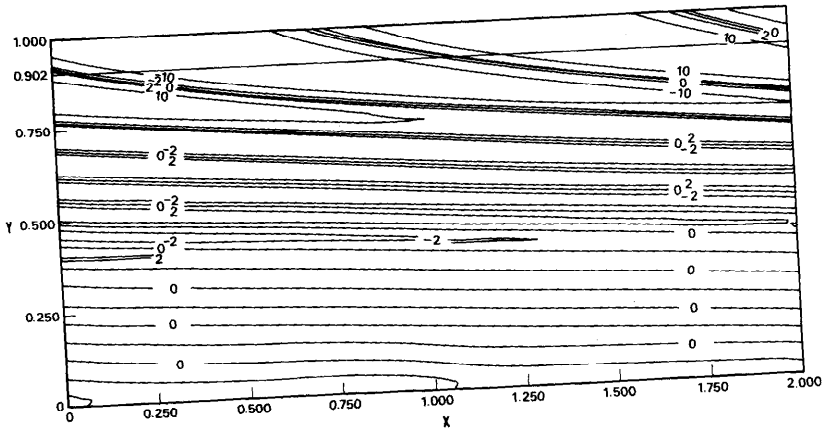

Fig. 7.7(a). Iso-vorticity curves for $E = 0.0100$, $M = 20.00$, $(R, W) = (200, 2)$.

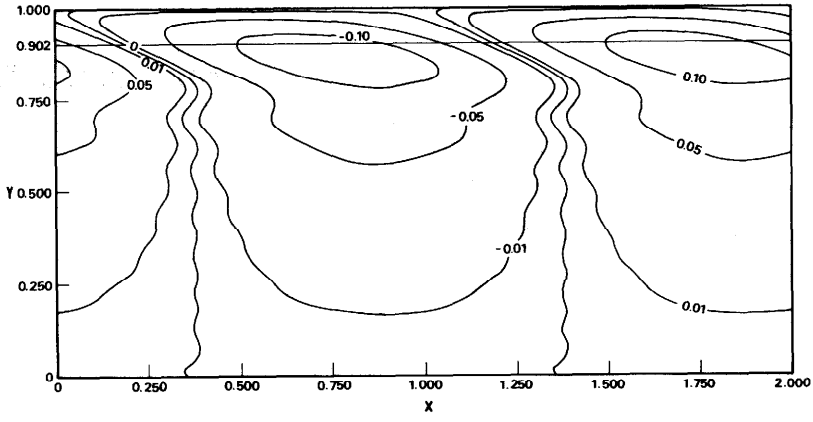

Fig. 7.7(b). Streamlines for $E = 0.0100$, $M = 20.00$, $(R, W) = (200, 2)$.

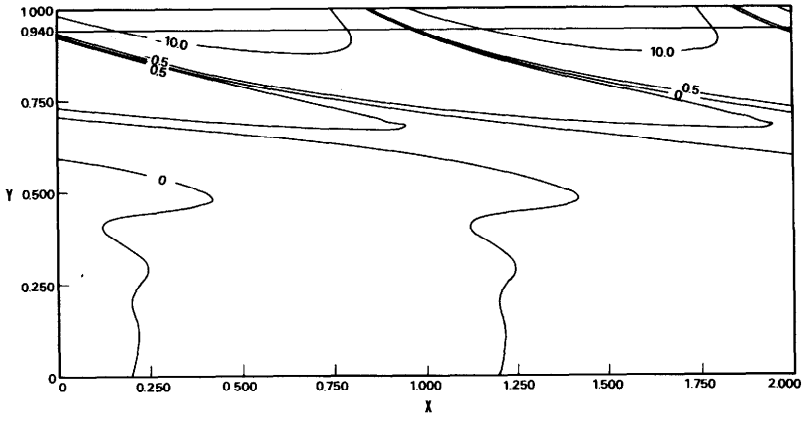

Fig. 7.8(a). Iso-vorticity curves for $E = 0.0010$, $M = 10.00$, $(R, W) = (316, 0.316)$.

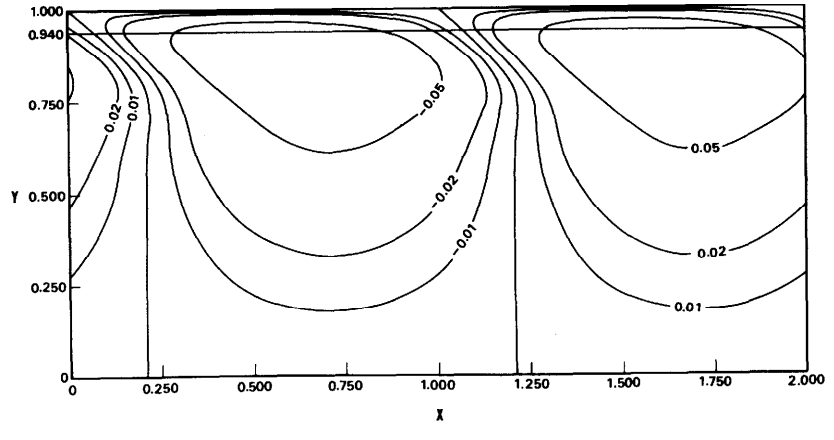

Fig. 7.8(b). Streamlines for $E = 0.0010$, $M = 10.00$, $(R, W) = (316, 0.316)$.

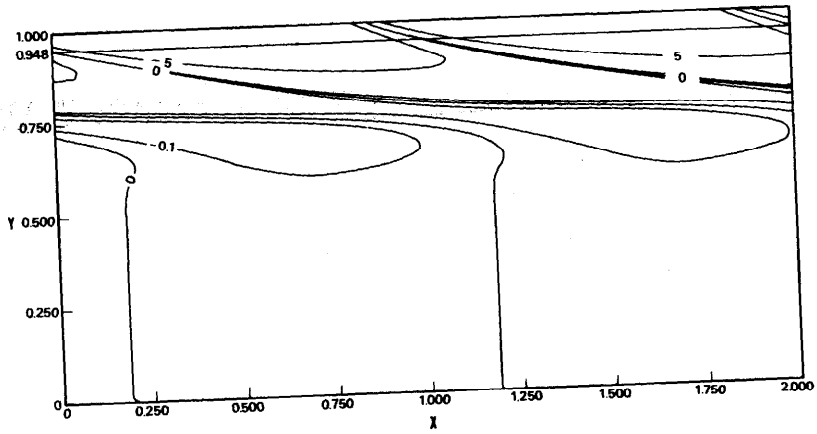

Fig. 7.9(a). Iso-vorticity curves for $E = 0.0001$, $M = 10.00$, $(R, W) = (1000, 0.1)$.

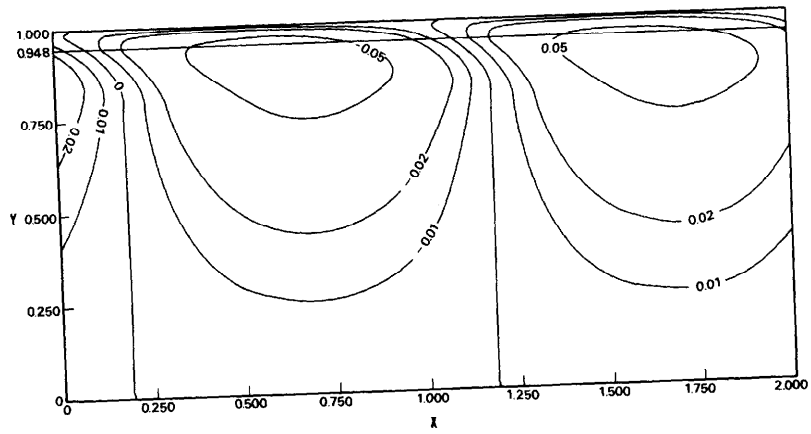

Fig. 7.9(b). Streamlines for $E = 0.0001$, $M = 10.00$, $(R, W) = (1000, 0.1)$.

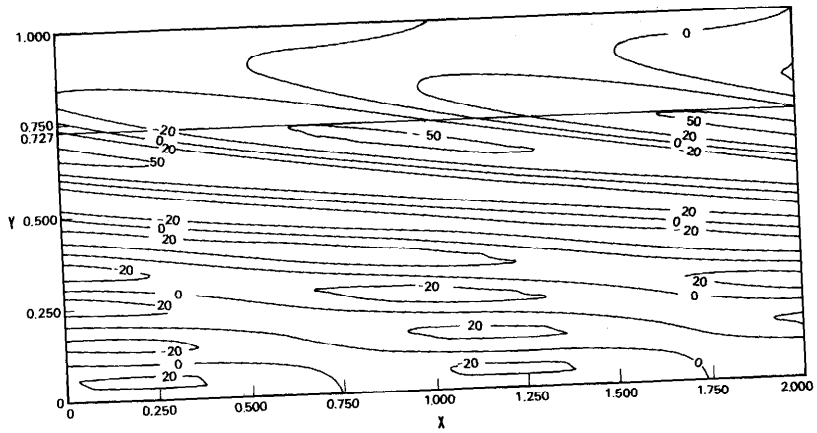

Fig. 7.10(a). Iso-vorticity curves for $E = 0.1000$, $M = 10.00$, $(R, W) = (31.6, 3.16)$.

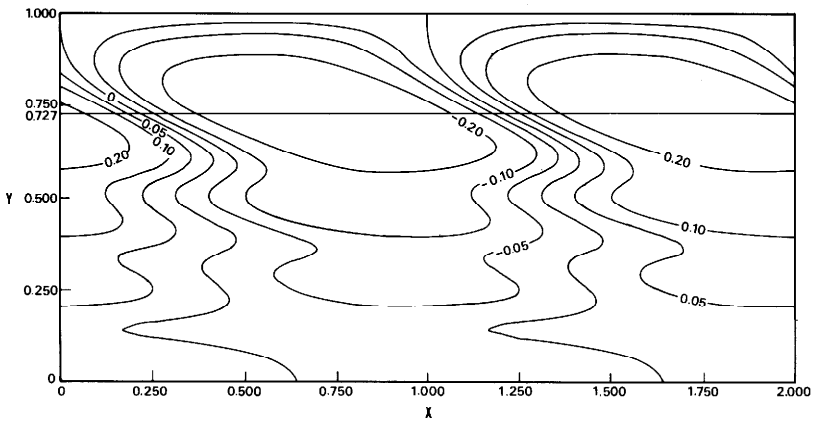

Fig. 7.10(b). Streamlines for $E = 0.1000$, $M = 10.00$, $(R, W) = (31.6, 3.16)$.

Figure 7.4 is representative of subcritical flow ($M < 1$). There is no strong shift in the phase of the perturbing data at the boundary. The lines of zero vorticity and the zero streamlines do not deviate strongly from the vertical. We draw attention to the difference between the iso-vorticity curves shown in Fig. 7.4 and the supercritical case which is exhibited in all the other figures.

The iso-vorticity curves in the supercritical cases shown in Figs. 7.5(a)–7.10(a) are dominated by the hyperbolic structure of the solution. The positive and negative vorticity are swept out along characteristics (shown in Figs. 7.1–7.3) in a manner already described. In Figs. 7.4–7.7 we have fixed $E = 0.01$ and increased M (or $W = M\sqrt{E}$). The damping of the vorticity decreases as W (or M) is increased. For larger values of M an oscillatory variation of the vorticity persists all the way to the channel center. The frequency of the oscillation increases with M (or W) at a fixed E. This property of damping is most clearly brought by comparing Figs. 7.6(a), 7.8(a), and 7.9(a). In these figures $M = 10$ is fixed and $E = 0.01$, 0.001, 0.0001, respectively. The damping is more rapid for the small values of E and the channel core is essentially free of perturbation vorticity.

Acknowledgements

This work was supported by the United States Army under Contract No. DAAG-29-82-K0051, by the Fluid Mechanics Branch of the National Science Foundation and by the Ministry of Education of the Republic of Korea and by the Korea Science and Engineering Foundation.

References

1 D.D. Joseph, M. Renardy and J.C. Saut, Hyperbolicity and change of type in the flow of viscoelastic fluids, Arch. Ration. Mech. Anal., 87(3) (1985) 213–251.
2 I.M. Rutkevich, The propagation of small perturbations in a viscoelastic fluid, J. Appl. Math. Mech., 34 (1970) 35–50.
3 I.M. Rutkevich, On the thermodynamic interpretation of the evolutionary conditions of the equations of the mechanics of finitely deformable viscoelastic media of Maxwell type, J. Appl. Math. Mech., 36 (1972) 283–295.
4 J.S. Ultman and M.M. Denn, Anomalous heat transfer and a wave phenomenon in dilute polymer solutions, Trans. Soc. Rheol., 14 (1970) 307–317.
5 M. Luskin, On the classification of some model equations for viscoelasticity. J. Non-Newtonian Fluid Mech, 16 (1984) 3–11.
6 J.Y. Yoo, M. Ahrens and D.D. Joseph, Hyperbolicity and change of type in sink flow. J. Fluid Mech., 153 (1985) 203–214.
7 J.C. Saut and D.D. Joseph, Fading memory, Arch. Ration. Mech. Anal., 81 (1983) 53–95.
8 A. Narain and D.D. Joseph, Linearized dynamics for step jumps of velocity and displacement of shearing flows of a simple fluid, Rheol. Acta, 21 (1982) 228–250.
9 A. Narain and D.D. Joseph, Remarks about the interpretation of impulse experiments in shear flows of viscoelastic liquids, Rheol. Acta, 22 (1983) 528–538.
10 A.B. Metzner, E.A. Uebler and C.F.C.M. Fong, Converging flows of viscoelastic materials, AIChE J., 15(5) (1969) 750–758.
11 A.G. Dodson, P. Townsend and K. Walters, On the flow of Newtonian and non-Newtonian liquids through corrugated pipes, Rheol. Acta, 10 (1971) 508–516.
12 L. Sturges, Secondary motion induced by the rotation of a wavy rod, Rheol. Acta., 16 (1977) 476–483.